

NMR Kinetic Investigations of the Photochemical and Thermal Reactions of a Photochromic Chromene

Stéphanie Delbaere,^{*,†} Jean-Claude Micheau,[‡] and Gaston Vermeersch[†]

Laboratoire de Physique et LARMN, UMR CNRS 8009, Faculté de Pharmacie, Université de Lille 2, F-59006 Lille, France, and Laboratoire IMRCP, UMR CNRS 5623, Université Paul Sabatier, F-31062 Toulouse, France

sdelbaer@pharma.univ-lille2.fr

Received September 2, 2003

The photochromic behavior of 2,2-di(4-fluorophenyl)-6-methoxy-2*H*-1-chromene has been investigated by ¹⁹F NMR spectroscopy. Photocoloration under UV irradiation at low temperature led to the formation of three interconverting photoisomers including two merocyanines and an unprecedented allenyl-phenol isomer. Photobleaching with visible light, which was known to lead to reversion to the initial closed chromene, was shown to increase allenyl-phenol concentration. Thermal relaxation of the preirradiated system was also studied at various temperatures. In each case (UV and visible irradiations, thermal isomerization), the kinetics of each of the four species was monitored. Numerical analysis of concentration vs time profiles enabled us to unequivocally establish the global mechanism occurring in each of the experimental conditions and to interpret the specific reactivity of each photoisomer. It has been shown that, among the 12 possible isomerization processes, only some paths were active. For the first time, it has been possible to determine their corresponding thermal activation parameters and photochemical quantum yield ratios.

Introduction

Photochromic molecules have received great attention in recent years due to their potential applications in variable transmission glasses, in high-density optical storage and switching, and in some attempts to manufacture light-driven molecular motors.^{1–5} However, the mechanisms used by multi-isomeric photochromic compounds remain unclear. Among photochromic molecules involving multi-isomeric systems, benzopyrans (also known as chromenes) are a promising class of compounds. Becker and Michl first reported them in 1966.⁶ UV irradiation of the colorless chromene proceeds through C–O bond cleavage, producing a distribution of orange to red isomeric open forms (merocyanines), which are thought to be thermally and/or photochemically reverted to the original benzopyran. In the presence of such complex systems, multiwavelength absorbance vs time matrixes are not a sufficient source of mechanistic information⁷ because spectral overlapping between sev-

eral photoisomers impedes the unequivocal extraction of the photoconversion quantum yields and molar absorption coefficients.

Recently, by use of ¹⁹F high-resolution NMR spectroscopy, we showed that irradiation of the 2,2-di(4-fluorophenyl)-6-methoxy-2*H*-1-chromene (FC or fluorochromene) generated, besides the two expected open merocyanines (the transoid-cis (TC) and the transoid-trans (TT) forms), an *o*-allenyl-*p*-methoxyphenol (AP).⁸ This compound had never been detected by any other method before, despite numerous investigations on benzo- and naphthopyran compounds.^{9–18} We think that it is worth investigating the kinetic behavior of this photochromic benzopyran since the involvement of an allenyl-phenol side product (AP) has recently been demonstrated to be

* To whom correspondence may be addressed. Fax: 333 2095 9009. Tel: 333 2096 4023.

[†] Université de Lille 2.

[‡] Université Paul Sabatier.

(1) Bertelson, R. C. In *Photochromism*; Brown, G. H., Ed.; Wiley: New York, 1971; pp 45–ff and references therein.

(2) Guglielmetti, R. In *Photochromism: Molecules and Systems, Studies in Organic Chemistry 40*; Dürr, H., Bouas-Laurent, H. Eds.; Elsevier: Amsterdam, 1990; Chapters 8 and 23 and references therein.

(3) Van Gemert, B. In *Organic Photochromic and Thermochromic compounds*; Crano, J. C., Guglielmetti, R. J., Eds.; Plenum Press: New York, 1999; Vol. 1, pp 111–140.

(4) Berkovic, G.; Krongauz, V.; Weiss, V. *Chem. Rev.* **2000**, *100*, 1741–1753.

(5) Koumura, N.; Zijlstra, R. W. J.; Van Delden, R. A.; Harada, N.; Feringa, B. L. *Nature* **1999**, *401*, 152–155.

(6) Becker, R. S.; Michl, J. *J. Am. Chem. Soc.* **1966**, *88*, 5931–5933.

(7) Metelitsa, A. V.; Micheau, J. C.; Voloshin, N. A.; Voloshina, E. N.; Minkin, V. I. *J. Phys. Chem. A* **2001**, *105*, 8417–8422.

(8) Delbaere, S.; Micheau, J.-C.; Vermeersch, G. *Org. Lett.* **2002**, *4*, 3143–3145.

(9) Becker, R. S.; Dolan, E.; Balke, D. *J. Chem. Phys.* **1969**, *50*, 239–245.

(10) Tyer, N. W.; Becker, R. S. *J. Am. Chem. Soc.* **1970**, *92*, 1289–1294.

(11) Kolc, J.; Becker, R. S. *Photochem. Photobiol.* **1971**, *13*, 423–429.

(12) Lenoble, C.; Becker, R. S. *J. Photochem.* **1986**, *33*, 187–197.

(13) Van Gemert, B.; Bergomi, M.; Knowles, D. *Mol. Cryst. Liq. Cryst.* **1994**, *246*, 67–73.

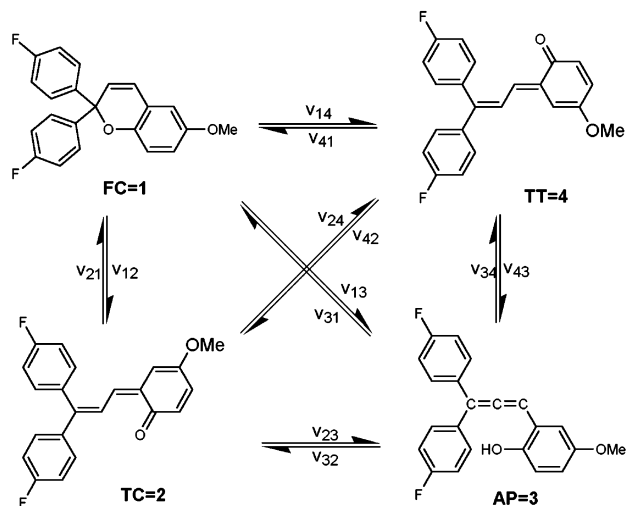
(14) Aldoshin, S.; Chuev, I.; Filipenko, O.; Lokshin, V.; Pozzo, J. L.; Pepe G.; Samat, A. *Acta Crystallogr. C* **1996**, *52*, 1537–1539.

(15) Ottavi, G.; Favaro, G.; Malatesta, V. *J. Photochem. Photobiol. A* **1998**, *115*, 123–128.

(16) Ortica, F.; Levi, D.; Brun, P.; Guglielmetti, R.; Mazzucato, U.; Favaro, G. *J. Photochem. Photobiol. A* **2001**, *139*, 133–141.

(17) Jockusch, S.; Turro, N. J.; Blackburn, F. R. *J. Phys. Chem. A* **2002**, *106*, 9236–9241.

(18) Zhao, W.; Carreira, E. M. *J. Am. Chem. Soc.* **2002**, *124*, 1582–1583.

SCHEME 1. Mechanistic Model Showing All the Possible Interconversion Paths between the Four Isomers^a


^a v_{ij} are the apparent rates. For the sake of clarity, FC = 1, TC = 2, AP = 3, TT = 4.

general as it has also been reported in nonfluorinated compounds.¹⁹ The kinetics of this fluorochromene were investigated at low temperature under continuous UV and visible irradiation, while thermal relaxations in the dark at various temperatures have also been monitored. The purpose of these experiments was to obtain very accurate concentration vs time profiles, from which we carried out an extended kinetic analysis to identify the isomeric forms and to determine which isomerization pathways occurred in a given experimental situation. In previous works, there are several examples of interconversion processes between photochromic isomers,^{20–23} but a quantitative analysis of a four-species photochromic system has, until now, never been published. For this purpose, we considered that Scheme 1 was the most general form for a four-isomer system in which every component—the 2,2-di(4-fluorophenyl)-6-methoxy-2H-1-chromene (FC), the two open merocyanines (TC and TT), and the AP—is assumed to react either thermally or photochemically to form every other component.²⁴

Such four-component interconverting systems have been used to describe enzyme folding²⁵ in biochemical literature. They are modeled by a set of linear differential equations

$$\frac{d[X_i]}{dt} = \sum_{m=1}^4 v_{mi} - \sum_{m=1}^4 v_{im} \quad i = 1-4 \text{ and } m \neq i \quad (1)$$

giving rise to multiexponential relaxations.

(19) Delbaere, S.; Vermeersch, G. *J. Photochem. Photobiol. A* **2003**, *159*, 227–232.

(20) Hobley, J.; Malatesta, V.; Millini, R.; Giroladini, W.; Wis, L.; Goto, M.; Kishimoto, M.; Fukumura, H. *Chem. Commun.* **2000**, 1339–1340.

(21) Chuev, I.; Aldoshin, S.; Samat, A.; Maurel, F.; Aubard, J. *THEOCHEM* **2001**, *548*, 123–132.

(22) Görner, H.; Chibisov, A. K. *J. Photochem. Photobiol. A* **2002**, *149*, 83–89.

(23) Rini, M.; Holm, A. K.; Nibbering, J.; Fidler, H. *J. Am. Chem. Soc.* **2003**, *125*, 3028–3034.

(24) Matsen, F. A.; Franklin, J. L. *J. Am. Chem. Soc.* **1950**, *72*, 3337–3341.

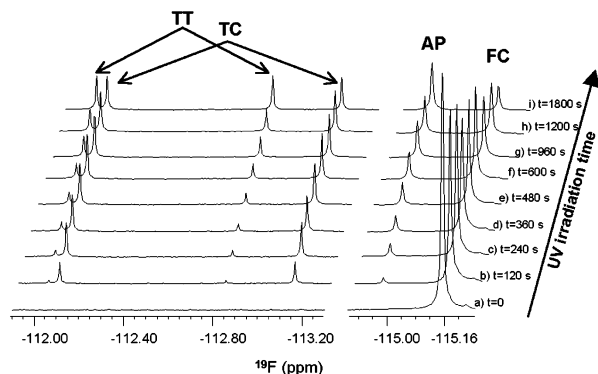


FIGURE 1. ¹⁹F NMR spectra of FC (−115.16) at 228 K. The times indicated are the cumulated periods of UV irradiation. The photoisomers produced are TT (−112.00; −112.80), TC (−112.06; −113.11), and AP (−114.94 ppm).

However, if the isomerizations are photochemically induced, it is possible that inner filter effects induce variations in the photokinetic factor, so giving rise to more complex kinetic rate laws. We have shown that the use of simultaneous nonlinear least-squares fitting of the four-species concentration vs time profiles provides unambiguous information about the location and the relative strengths of the various photochemical and thermal isomerization pathways.

In this paper, on the basis of Scheme 1, we quantitatively analyzed all the possible photochemical and thermal isomerization processes among the four identified long-lived fluorine-containing species, which are able to accumulate sufficiently.²⁶

Results and Discussion

UV and Visible Irradiation at Low Temperature. The UV irradiation of a solution of 2,2-di(4-fluorophenyl)-6-methoxy-2H-1-chromene (FC) in acetonitrile-*d*₃ was investigated at 228 K. At this temperature, there is no noticeable thermal isomerization, so the evolution in the photochromic system (the solution turns red) can only be attributed to UV-induced photochemical processes. Figure 1 shows the successive ¹⁹F NMR spectra recorded under UV irradiation. The various photoisomers (photochromerocyanine TT, TC, and AP) increase while the starting FC decreases.⁸

In our experimental conditions, fluorine atom mass balance was spontaneously respected and degradation was negligible (i.e., less than 2%). The plots of the photocoloration kinetics (Figure 2) show the simultaneous evolution of the four isomeric species FC, TC, AP, and TT. From this plot, homemade software^{27–29} was used to perform kinetic analysis on the basis of Scheme 1. The calculated evolution in concentrations was obtained by numerical integration of the set of differential equations

(25) Bieri, O.; Wildegger, G.; Bachmann, A.; Wagner, C.; Kieflhaber, T. *Biochemistry* **1999**, *38*, 12460–12470.

(26) Aubin, L. B.; Wagner, T. M.; Thoburn, J. D.; Kesler, B. S.; Hutchinson, K. A.; Schumaker, R. R.; Parakka, J. P. *Org. Lett.* **2001**, *3*, 3413–3416.

(27) Kaps, K.; Rentrop, P. *Comput. Chem. Eng.* **1984**, *8*, 393–396.

(28) Minoux, M. In *Programmation Mathématique*; Dunod, Ed.; Bordas: Paris, 1983; Vol. 1, pp 95–168.

(29) Deniel, M. H.; Lavabre, D.; Micheau, J. C. In *Organic Photochromic and Thermodynamic Compounds*; Crano, J. C., Guglielmetti, R., Eds.; Plenum Press: New York, 1999; Vol. 2, pp 167–209.

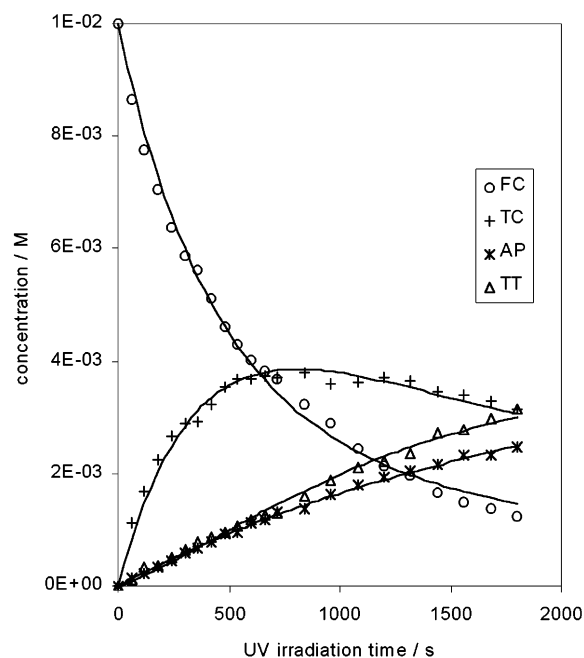


FIGURE 2. Photocoloration kinetics under UV irradiation (signs are experimental concentrations, solid lines are best fits from our model).

(eq 1). The photochemical rates³⁰ v_{ij} are given by

$$v_{ij} = \Phi_{ij} \epsilon_i I_0 F [X_i] = h_{ij} [X_i] \quad (2)$$

By minimization of the residual quadratic error χ^2 between the calculated and the NMR measured experimental concentrations, only those processes remained which were kinetically significant, indicating the location of the photochemical pathways and delivering the corresponding values of h_{ij} . We found that the fitting procedure was very selective among the various possible processes. The simulated kinetic curves were significantly distant from their corresponding experimental data if some important parameter was omitted or if the presence of a forbidden pathway was artificially imposed (see Supporting Information for the details). Results are grouped in Scheme 2 and Table 1.

Close examination of the results in Table 1 shows that the major part of the photochemical reactivity of FC concerns its photoconversion to TC. UV irradiation causes C–O bond cleavage, leading to a sterically crowded cisoid isomer through a zwitterionic intermediate³² (non-monitorable under our conditions) whose further rearrangement gives rise to TC. This path requires only a C₃–C₄ one-bond rotation. From FC, minor paths to AP

(30) Φ_{ij} is the quantum yield of the photochemical transformation of compound "X_i" into compound "X_j", ϵ_i is the molar absorption coefficient of compound X_i at the irradiation wavelength, l is the optical path, I_0 is the incident photon flux, and F is the photokinetic factor. Its variations during the UV irradiation period have been neglected. This assumption is fully justified as F is strictly constant when the irradiation wavelength is close to an isosbestic point or if the absorbance of the photochemical reacting solution is sufficiently low. As the irradiation light was not strictly monochromatic, Φ_{ij} and ϵ_i values must be considered as wavelength averaged. Then h_{ij} terms correspond to apparent first-order rate constants.

(31) Relative errors for the stated parameters v_{ij} are estimated to be less than $\pm 5\%$ for the most sensitive (or $\pm 10\%$ for the corresponding ratios).

(32) Kolc, J.; Becker, R. S. *J. Phys. Chem.* **1967**, *12*, 4045–4048.

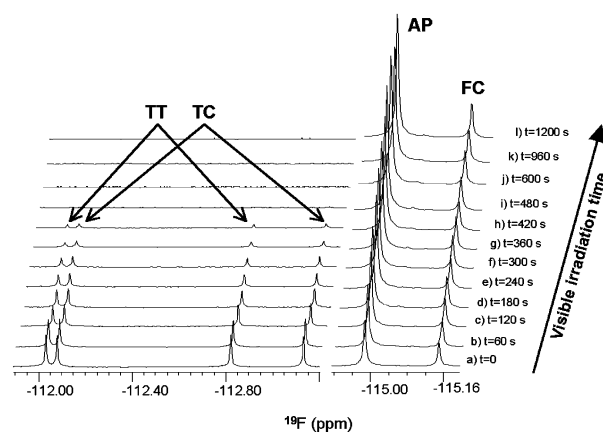
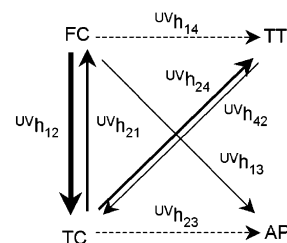


FIGURE 3. ¹⁹F NMR spectra of the photochromic mixture at 228 K during visible irradiation. The initial spectrum ($t = 0$) corresponds to the end of UV irradiation. The times indicated are the cumulated periods of visible light irradiation.

SCHEME 2. Photoisomerization Processes Occurring under UV Irradiation at 228 K^a



^a The sizes of the arrows give a rough indication of the relative quantum yield values.

TABLE 1. Apparent Photochemical Rates and Relative Wavelength-Averaged Quantum Yields for Processes Occurring under UV Irradiation³¹

process	apparent photochemical rate constants	relative quantum yields	
		from FC	from TC
FC → TC	$UVh_{12} = 1.50 \times 10^{-3}$	0.81	
FC → AP	$UVh_{13} = 2.16 \times 10^{-4}$	0.12	
FC → TT	$UVh_{14} = 1.30 \times 10^{-4}$	0.07	
TC → FC	$UVh_{21} = 6.22 \times 10^{-4}$		0.46
TC → AP	$UVh_{23} = 1.83 \times 10^{-4}$		0.13
TC → TT	$UVh_{24} = 5.50 \times 10^{-4}$		0.41
TT → TC	$UVh_{42} = 3.48 \times 10^{-4}$		

and TT are also observed. On the other hand, absorption of UV by TC induces the reverse reaction, i.e., ring closure to FC. Also of importance is bond rotation around C₄–C_{4a}, leading to the second merocyanine transoid isomer TT. There is also a minor path to AP. As Φ_{AP}/Φ_{TT} from FC = $1.66 \neq \Phi_{AP}/\Phi_{TT}$ from TC = 0.33, it is likely that there is no common intermediate from FC and TC to TT and AP. As for TT, it was found that its only photochemical isomerization was the C₄–C_{4a} bond rotation to TC. More interesting is the complete lack of photoreactivity from the newly discovered AP that is likely to be an indication of some forbidden photochemical pathways.

Under visible light irradiation, the red solution is bleached and, as illustrated in Figure 3, TC and TT gradually disappear while AP increases.

Careful observation of the concentration vs time kinetic curves (Figure 4) shows that only the two photomero-

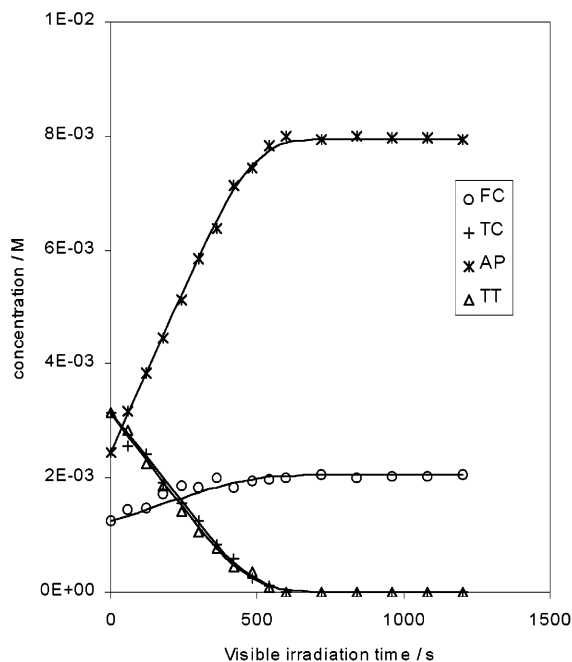
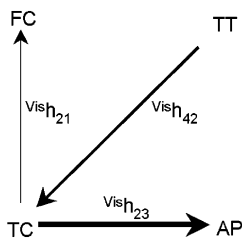


FIGURE 4. Photobleaching kinetics under visible light irradiation (signs are experimental concentrations, solid lines are best fits from our model).

SCHEME 3. Photoisomerization Processes Occurring under Visible Light Irradiation at 228 K^a



^a The sizes of the arrows give a visual indication of the relative values of the corresponding quantum yields.

cyanines TC and TT were photoreactive but that they did not follow mono- or multiexponential decays. They appeared as zero order. This particular kinetic feature has been accounted for by a strong variation in photokinetic factor throughout visible irradiation.³³

Only three photoisomerization paths were detected: TC → FC, TC → AP, and TT → TC, confirming, as expected, that FC and AP are not reactive under visible irradiation due to the lack of visible absorption. (Scheme 3 and Table 2).

The predominant reaction appears to be the photoenolization of TC (TC → AP). This reaction is likely to occur via a [1,5]-hydrogen shift. In the TC isomer, this rearrangement is possible because there is a helical trienic open chain (H₃C₃C₄C_{4a}C_{8a}O), in which continuous overlap can be maintained. Such geometrical requirements are

(33) In the photokinetic factor $F = (1 - 10^{-Abs'})/Abs'$, Abs' is the total absorbance of the sample at the irradiation wavelength. If the photoproducts do not absorb at the irradiation wavelength, the photochemical rate reduces to $v_{ij} = \Phi_{ij} I_0 (1 - 10^{-Abs'})$ with $Abs' = (\epsilon'_{TC}[TC] + \epsilon'_{TT}[TT])l$. In the first part of the evolution, as TC and TT remain sufficiently high, the term $10^{-Abs'} \rightarrow 0$ while $\rightarrow 1$ in the final part, hence the zero-order-like kinetics.

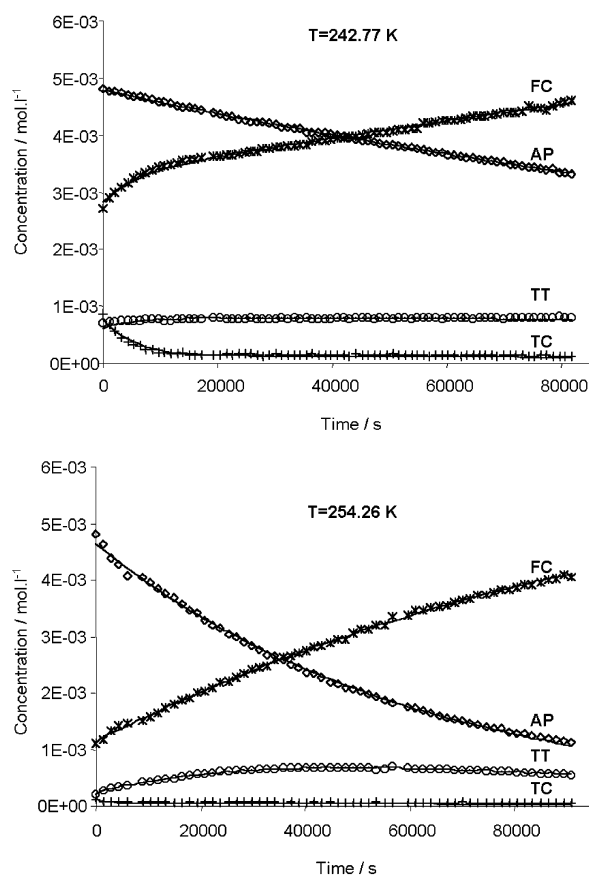


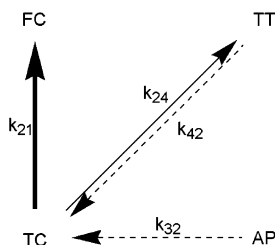
FIGURE 5. Time evolution of concentrations of FC, TC, AP, and TT at two different temperatures. Dots are experimental data; continuous lines are fitted curves from the Scheme 4 model.

TABLE 2. Apparent Photochemical Rate Constants and Wavelength-Averaged Relative Quantum Yields from TC under Visible Irradiation

process	apparent photochemical rate constants	relative quantum yields from TC
TC → AP	$Vis h_{23} = 1.20 \times 10^{-2}$	0.87
TC → FC	$Vis h_{21} = 1.79 \times 10^{-3}$	0.13
TT → TC	$Vis h_{42} = 7.22 \times 10^{-3}$	

not possible within the TT structure. The absence of photochemical pathway from TT → AP can then be justified. The marked differences between TC reactivities under UV and visible light (Φ_{FC}/Φ_{AP})_{UV} = 3.40 and (Φ_{FC}/Φ_{AP})_{vis} = 0.15 can be accounted for by the presence of various vibrational levels within the excited state. The visible photon only makes it possible to reach a less energetic state from which ring closure to FC is less favorable. Also less favorable is the photoisomerization TC → TT, which was not detected under visible irradiation.

Thermal Relaxations. When kept in the dark at higher temperatures, there was slow but complete disappearance of both merocyanines TT and TC and AP as well as recovery of the initial FC. The recorded kinetics of the thermal relaxation processes after UV + visible irradiation (Figure 5) show the influence of temperature on the relative amplitude and curvatures of the concentration vs time profiles.

SCHEME 4. Thermal Processes Occurring during Relaxation^a


^a The sizes of the arrows are a visual indication of the relative values of the corresponding rate constants.

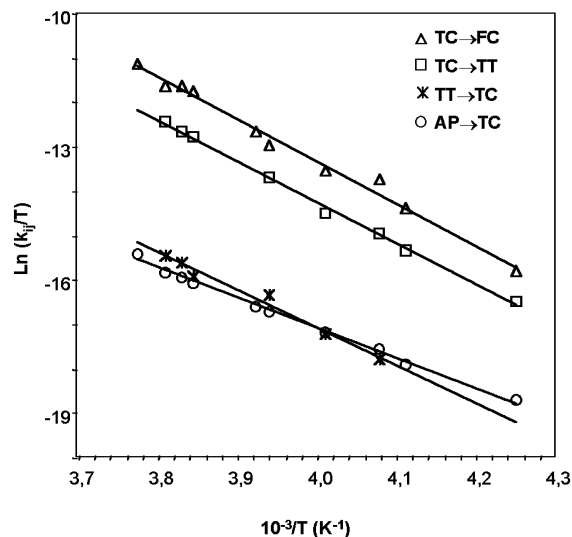


FIGURE 6. Eyring plots for the four thermal relaxation processes.

These kinetics were also analyzed according to general Scheme 1 where the rates v_{ij} were considered as thermal terms, being equal to $k_{ij}[X_i]$ where k_{ij} are the corresponding first-order rate constants. Numerical fitting of the whole set of kinetics showed that only four paths (among the possible 12) were needed to account for all the various temperature kinetic results. AP undergoes a slow irreversible process to TC. TC is the only structure able to be converted directly to FC by a single bond rotation and acts as a key intermediate in the pathway from AP to FC. On the contrary, the TT isomer, needing a double bond rotation for reversion, does not proceed directly to FC. The slightly transient TT concentration increase indicates a slow equilibration process with TC (Scheme 4).

From the Eyring plots $\ln(k_{ij}/T)$ vs $1/T$ (Figure 6), the standard entropy and enthalpy of activation, ΔS^\ddagger and ΔH^\ddagger , respectively, were obtained (Table 3).

The enthalpy of activation values agree with those generally obtained for photochromic compounds (from about 40 to 120 kJ mol⁻¹).^{1,2,34} The highest ΔH^\ddagger values correspond to processes coming from TC, while the lowest corresponds to processes going to TC. ΔS^\ddagger values are more difficult to interpret. This parameter can be considered as the sum of two contributions: $\Delta S^\ddagger_{\text{intr}}$ from the reaction

TABLE 3. Standard Entropy and Enthalpy of Activation, ΔS^\ddagger and ΔH^\ddagger , Calculated from Eyring's Equation

processes	ΔS^\ddagger (J mol ⁻¹ K ⁻¹)	ΔH^\ddagger (kJ mol ⁻¹)
TC → TT	27.5 ± 2.1	85.6 ± 4.2
TC → FC	20.7 ± 0.8	82.2 ± 2.2
TT → TC	-61.3 ± 8.7	69.4 ± 5.0
AP → TC	-106.7 ± 6.2	58.3 ± 1.3

itself and $\Delta S^\ddagger_{\text{solv}}$ from the rearrangement of the solvent.

$$\Delta S^\ddagger = \Delta S^\ddagger_{\text{intr}} + \Delta S^\ddagger_{\text{solv}} \quad (3)$$

Moreover, it can be argued that polar acetonitrile is more oriented near polar open forms than near the less polar closed forms. Higher positive $\Delta S^\ddagger_{\text{solv}}$ are therefore expected during the open to closed reactions rather than during open to open rearrangements. This is a possible explanation for the positive value found for the open to closed TC → FC process. Among the remaining processes, the lowest negative activation entropy is for AP → TC isomerization. This reaction has already been shown in a previous paper³⁵ to occur via a [1,5]-sigmatropic hydrogen shift. According to the Woodward–Hoffmann rules for sigmatropic rearrangements,^{36,37} the [1,5] migration of hydrogen involves a six-membered-ring (i.e., highly ordered) transition state in accordance with the highly negative $\Delta S^\ddagger_{\text{intr}}$. Because an odd number (3) of pairs of electrons (two π bonds and a pair of π electrons) are involved, the ground-state HOMO is symmetrical. Then, the selection rules require that the [1,5]-hydrogen shift suprafacial rearrangement occurs under thermal conditions and is forbidden under photochemical conditions in complete agreement with our conclusions (AP → TC is thermal but not photochemical).

Analysis of the variations of the TC → TT (k_{24}) and TT → TC (k_{42}) rate constants enabled us to estimate the relative thermodynamic stability of the two photomerocyanine isomers. Although the equilibrium between TT and TC was never reached in our experimental conditions, the expected equilibrium constant can be calculated from the kinetic rate constants of the reversible process. We obtained a value $[\text{TT}]/[\text{TC}]_{\text{eq}} = k_{24}/k_{42} = K_{\text{eq}}$, which lies between ca. 15 and 50, depending on the temperature. This result confirms that the TT conformation is more stable than the TC and that the free enthalpy ΔG° is around 6.5 kJ mol⁻¹ at 260 K.

Conclusions

For the first time, photocoloration under UV, photobleaching by visible light, and thermal bleaching of a fluorinated photochromic benzopyran have been investigated by ¹⁹F NMR spectroscopy. UV excitation of ring-closed FC yields TC and TT merocyanine isomers, as well as AP. On the basis of a quantitative measurement of concentrations and subsequent numerical kinetic analysis using a without a priori model, the most plausible

(35) Delbaere, S.; Micheau, J.-C.; Teral, Y.; Bochu, C.; Campredon, M.; Vermeersch, G. *Photochem. Photobiol.* **2001**, *74*, 694–699.

(36) Woodward, R. B.; Hoffmann, R. *J. Am. Chem. Soc.* **1965**, *87*, 395–397.

(37) Woodward, R. B.; Hoffmann, R. *J. Am. Chem. Soc.* **1965**, *87*, 2511–2513.

(34) Hopley, J.; Malatesta, V. *Phys. Chem. Chem. Phys.* **2000**, *2*, 57–59.

mechanism was deduced and the values of the relative quantum yields were extracted. It was found that under UV, the main photochemical process is the TC \rightarrow FC photoequilibrium.

However, both compounds also undergo some minor rearrangements to TT and AP. AP has been shown not to be photochemically reactive. Under visible light, only the two merocyanines TT and TC are photochemically reactive. TC is converted to both AP and ring-closed chromene FC. Merocyanine TT is only photoisomerized to TC.

Thermal bleaching relaxation was extensively studied at various temperatures. The main path is isomerization of the AP to the ring-closed chromene FC. This path occurs in two steps, TC playing the role of intermediate. But, TC has also been found to be involved in a pseudo-equilibrium with TT. The relative stability of the two photomerocyanines TC and TT has been determined, TT conformation being more stable than TC. We think that these results possess a general character and apply whatever the detailed structure of the chromene under investigation. Our conclusions will undoubtedly open the way to further theoretical modeling of the chromene photochromic reaction.

Experimental Section

Samples ($[FC]_0 = 10^{-2}$ mol L $^{-1}$ in CD $_3$ CN) were irradiated directly in the NMR tube (5 mm) using a 1000 W Xe–Hg high-pressure filtered short-arc lamp (Oriel), equipped with ad-

equate filters (Schott 011FG09, $259 < \lambda < 388$ nm with $\lambda_{\max} = 330$ nm for UV irradiation, and Oriel 3–74, $\lambda > 400$ nm for visible irradiation). Temperature was regulated with a home-built apparatus described elsewhere.³⁴ After irradiation, the sample was transferred into the thermoregulated probe of a Bruker Avance-DPX NMR spectrometer (^1H , 300 MHz; ^{19}F , 282 MHz). ^1H and ^{19}F NMR spectra at 228 K were recorded. For thermal relaxation studies, only ^{19}F NMR spectra were recorded at regular intervals at higher selected temperatures (235, 242.8, 244.8, 248.9, 253.2, 254.3, 259.4, 260.4, 261.7, 264.2 K).

Acknowledgment. The 300-MHz NMR facilities were funded by the Région Nord-Pas de Calais (France), the Ministère de l'Éducation Nationale, de l'Enseignement Supérieur et de la Recherche, and the Fonds Européens de Développement Régional. We thank Dr. M. Campredon (University of Méditerranée) for the gift of fluoro-[2H]chromene. Part of this collaborative work was performed within the framework of the "Groupe de Recherche: Photochromes Organiques, Molécules, Mécanismes, Modèles", GDR CNRS No. 2466.

Supporting Information Available: UV spectrum of FC, ^1H and ^{19}F NMR spectra, and details of the data analysis and fitting procedure in PDF format. This material is available free of charge via the Internet at <http://pubs.acs.org>.

JO035279R